

# Hybridization-related correction to the jellium model for fullerenes

A V Verkhovtsev<sup>1,2</sup>, R G Polozkov<sup>2</sup>, V K Ivanov<sup>2</sup>, A V Korol<sup>1</sup>, A V Solov'yov<sup>1</sup>‡

<sup>1</sup> Frankfurt Institute for Advanced Studies, Ruth-Moufang-Str. 1, 60438 Frankfurt am Main, Germany

<sup>2</sup> St. Petersburg State Polytechnic University, Politekhnicheskaya ul. 29, 195251 St. Petersburg, Russia

E-mail: verkhovtsev@fias.uni-frankfurt.de

**Abstract.** We introduce a new type of a correction for a more accurate description of fullerenes within the spherically symmetric jellium model. This correction represents a pseudopotential which originates from the comparison between an accurate *ab initio* and the jellium model calculations. It is shown that such correction to the jellium model allows one to account, at least partly, for the  $sp^2$ -hybridization of carbon atomic orbitals. Therefore, it may be considered as a more physically meaningful correction as compared with a structureless square well pseudopotential which has been widely used earlier.

PACS numbers: 31.15.A-, 31.15.xr, 36.40.-c

## 1. Introduction

Since the discovery of fullerenes by Kroto *et al.* [1] in 1985, these compounds have been the objects of intensive experimental and theoretical investigations (see, e.g., [2]). At present, the investigation of fullerenes is active since they are proposed to be used in various fields of science and technology. One of the promising ideas is related to the possible application of fullerenes and their derivatives in medicine. For instance, they are proposed to be used as carriers in mechanisms of drug and gene delivery [3, 4] and thought to have potential antiviral activity which should have strong implications on the treatment of HIV-infection [5]. Excitation of fullerenes, placed in a biological medium, by an external radiation or incident heavy ions may lead to an active generation of secondary electrons or reactive oxygen species which allows fullerenes to be potentially used as sensitizers in photodynamic therapy [6]. A very important fundamental problem closely related to the mentioned applications is an adequate description of dynamic response of fullerenes to external fields or to the interaction with projectiles.

Contemporary software for the quantum-chemical calculations (e.g., Gaussian 09 [7]) provides an accurate quantitative description of the ground state of many-particle systems (fullerenes, in particular), and allows one to obtain information on geometrical and chemical properties of the system. Meanwhile, the description of

‡ On leave from A.F. Ioffe Physical Technical Institute, St. Petersburg, Russia

dynamic properties, which play an important role in the process of photoionization, by means of such programs faces significant difficulties. Dynamic properties (e.g., dynamic polarizability) are closely related to the response of a many-electron system to an external electromagnetic field. In many cases the properties are governed by a collective excitation of electrons and the formation of plasmon resonances in the excitation spectra [8]. In various systems plasmon resonances lie either below the ionization threshold (in metal clusters) or above it (e.g., in fullerenes). Out of these two classes of atomic clusters, only optical response of metal clusters has been calculated so far with the help of quantum-chemical programs (see, e.g. [9, 10]). Collective electron excitations in fullerenes, which lie in the continuous spectrum, have not been described so far by means of quantum-chemical programs. However, this can be achieved within simplified model approximations. As a compulsory starting point, these approximations must provide an accurate quantitative description of the ground state features of considered systems, in order to be applied to the investigation of the dynamic response and to the calculation of the photoabsorption (or, in particular, photoionization) spectrum.

One of the well-known and widely used approaches is based on the jellium model [11]. It was applied frequently to the description of ground state properties of metal clusters [11, 12, 13] and fullerenes [14, 19], as well as to the investigation of photoexcitation processes arising in these systems [15, 16, 17, 18, 19, 20, 21, 22, 23]. In the cited papers, the geometry of fullerenes was defined in two different ways: either as a infinitely thin sphere [19, 22] or as a spherical layer of a finite thickness [14, 17, 18, 20, 21, 23].

In [14, 24] it was stated that the ground state properties of fullerenes cannot be described properly by the standard jellium model which produces, in particular, unreliable values for the total energy [14]. To avoid this, adding of *structureless* pseudopotential corrections was suggested [14]. As a rule, a phenomenological square-well pseudopotential has been commonly used in the calculations [14, 17, 20, 23]. It was claimed that account for such pseudopotential increases the accuracy of the jellium-based description [17] and, for instance, allows one to reproduce the experimental value of the first ionization potential of  $C_{60}$  [23]. Meanwhile, the applicability of the jellium model for fullerenes and the choice of parameters of the used square-well pseudopotential have not been clearly justified so far from a physical viewpoint.

In the present paper we use another methodology and introduce a *structured* pseudopotential which originates from the comparison of an accurate *ab initio* calculation with the jellium-based one. Using this pseudopotential as a correction to the standard jellium model one can account, at least partly, for the  $sp^2$ -hybridization of carbon atomic orbitals and relate parameters of the jellium model with the features of the system obtained from the more precise calculation. By means of the presented pseudopotential, a relatively simple jellium model acquires more physical sense and parameters of the model obtain a clear physical justification. Hereby, we confirm the relevance of using the jellium model for the description of fullerenes. Investigating two molecules,  $C_{60}$  and  $C_{20}$ , we show that obtained results have a common origin and they could be also extended to other highly symmetric fullerenes.

The atomic system of units,  $m = |e| = \hbar = 1$ , is used throughout the paper.

## 2. Methods of investigation

### 2.1. Jellium model

In the present paper the fullerenes  $C_{60}$  and  $C_{20}$  are treated within the jellium model which is based on an assumption that a many-electron system is considered as a sum of two interacting subsystems: a valence electrons subsystem and that of a positively charged ionic core. Thus, a detailed ionic structure of the system is substituted with the uniform spherically symmetric distribution of the positive charge, in the field of which the motion of the valence electrons is considered [11].

The valence  $2s^2 2p^2$  electrons in each carbon atom form a cloud of delocalized electrons while the inner-shell  $1s^2$  electrons are treated as frozen and are not taken into consideration. Thereby, we consider 240 delocalized electrons in  $C_{60}$  and 80 electrons in  $C_{20}$ . The valence electrons are moving in a spherically symmetric central field, so one can construct the electronic configuration described by the unique set of quantum numbers  $\{n, l\}$  where  $n$  and  $l$  are the principal and orbital quantum numbers, respectively.

Since it is commonly acknowledged [25, 26, 27] that  $C_{60}$ , as well as other fullerenes, is formed from fragments of planar graphite sheets, it is natural to match the  $\sigma$ - and  $\pi$ -orbitals of graphite to the nodeless and the single-node wave functions of a fullerene, respectively [28]. Carbon atoms within a graphite sheet are connected by  $\sigma$ -bonds whereas different sheets are connected by  $\pi$ -bonds. In the fullerene, the nodeless  $\sigma$ -orbitals are localized at the radius of the ionic core while the single-node  $\pi$ -orbitals are oriented perpendicularly to the fullerene surface. The ratio of  $\sigma$ - to  $\pi$ -orbitals in  $C_{60}$  should be equal to 3 : 1 due to the  $sp^2$ -hybridization of carbon orbitals [29]. Thereby, the electronic configuration of the delocalized electrons in  $C_{60}$  is written in the form [19]:

$$1s^2 2p^6 3d^{10} 4f^{14} 5g^{18} 6h^{22} 7i^{26} 8k^{30} 9l^{34} 10m^{18} \\ 2s^2 3p^6 4d^{10} 5f^{14} 6g^{18} 7h^{10}.$$

Radial wave functions of the  $1s \dots 10m$  shells are nodeless, while the wave functions of the  $2s \dots 7h$  shells have one radial node each.

Using the same methodology, one defines the electronic configuration of the 80 delocalized electrons in  $C_{20}$  as follows:

$$1s^2 2p^6 3d^{10} 4f^{14} 5g^{18} 6h^{10} 2s^2 3p^6 4d^{10} 5f^2.$$

One of the stable isomers of  $C_{20}$  corresponds geometrically to the regular dodecahedron [30] and, like the truncated icosahedron  $C_{60}$ , has the symmetry of the  $I_h$  point group which is very close to the spherical symmetry. Therefore, within the jellium model the fullerene core of the charged carbon ions,  $C^{4+}$ , is described as a positively charged spherical layer of a finite thickness  $\Delta R = R_2 - R_1$ . The potential of the core may be written as:

$$U_{\text{core}}(r) = -N \times \begin{cases} \frac{3}{2} \frac{R_2^2 - R_1^2}{R_2^3 - R_1^3}, & r < R_1 \\ \frac{1}{2(R_2^3 - R_1^3)} \left( 3R_2^2 - r^2 \left( 1 + \frac{2R_1^3}{r^3} \right) \right), & R_1 \leq r \leq R_2 \\ \frac{1}{r}, & r > R_2 \end{cases}, \quad (1)$$

where  $N$  is the number of delocalized electrons in a fullerene ( $N = 240$  in  $C_{60}$  and  $N = 80$  in  $C_{20}$ ),  $R_1 = R - \Delta R/2$  and  $R_2 = R + \Delta R/2$  with  $R$  standing for a fullerene

radius ( $R_{C_{60}} = 3.54 \text{ \AA}$  and  $R_{C_{20}} = 2.04 \text{ \AA}$  [31]). The thickness  $\Delta R$  is chosen to be equal to  $1.5 \text{ \AA}$  which corresponds to a typical diameter of a carbon atom [32] and refers to experimental data from [20].

The electronic subsystem is treated within the local density approximation (LDA). Single-electron wave functions  $\phi_{nlm}(\mathbf{r})$  and the corresponding energies  $\varepsilon_{nl}$  are determined from a system of self-consistent Kohn-Sham equations:

$$\left[ -\frac{\Delta}{2} + U_{\text{eff}}(\mathbf{r}) \right] \phi_{nlm}(\mathbf{r}) = \varepsilon_{nl} \phi_{nlm}(\mathbf{r}) , \quad (2)$$

$$U_{\text{eff}}(\mathbf{r}) = U_{\text{core}}(r) + \int \frac{\rho(\mathbf{r}')}{|\mathbf{r} - \mathbf{r}'|} d\mathbf{r}' + U_{\text{XC}}^{\text{LDA}}(\mathbf{r}) , \quad (3)$$

$$\rho(\mathbf{r}) = \sum_{nl} \sum_{m=-l}^l \frac{N_{nl}}{2(2l+1)} |\phi_{nlm}(\mathbf{r})|^2 , \quad (4)$$

where  $N_{nl}$  is a number of electrons in the  $nl$ -shell. Exchange-correlation potential  $U_{\text{XC}}^{\text{LDA}}(\mathbf{r})$  is represented as a sum of the Slater exchange potential and a correlation potential:

$$U_{\text{XC}}^{\text{LDA}}(\mathbf{r}) = U_{\text{X}}(\mathbf{r}) + U_{\text{C}}(\mathbf{r}) = - \left( \frac{3}{\pi} \right)^{1/3} \rho^{1/3}(\mathbf{r}) + U_{\text{C}}(\mathbf{r}) . \quad (5)$$

In the calculations, we used Perdew and Zunger parameterization of the correlation potential [33] which is presented in the form

$$U_{\text{C}}(r_s) = \varepsilon_{\text{C}}(r_s) \frac{1 + 1.229\sqrt{r_s} + 0.444r_s}{1 + 1.053\sqrt{r_s} + 0.333r_s} , \quad (6)$$

$$\varepsilon_{\text{C}}(r_s) = - \frac{0.142}{1 + 1.053\sqrt{r_s} + 0.333r_s} , \quad (7)$$

where  $r_s(\mathbf{r}) = (4\pi\rho(\mathbf{r})/3)^{-1/3}$  is the local Wigner-Seitz radius for the electronic subsystem and  $\varepsilon_{\text{C}}(r_s)$  is the correlation energy per one electron.

## 2.2. Ab initio calculations

The *ab initio* calculations were performed using Gaussian 09 package [7]. For the description of the  $C_{60}$  and  $C_{20}$  fullerenes we used the split-valence triple-zeta basis set 6-311+G(d) with an additional set of polarization and diffuse functions. The systems were calculated by means of the density functional theory. To account for the exchange and correlation corrections the Slater exchange functional [34] and the local Perdew functional (the so-called Perdew Local, PL) [33] were used. By applying these rather simple functionals we wanted to achieve a full similarity in the description of the electronic subsystem within the jellium model and the *ab initio* approaches.

The total electrostatic potential of the system is represented as a sum of the nuclear and electronic parts:

$$U_{\text{tot}}(\mathbf{r}) = U_{\text{n}}(\mathbf{r}) + U_{\text{el}}(\mathbf{r}) = - \sum_A \frac{Z_A}{|\mathbf{r} - \mathbf{R}_A|} + \int \frac{\rho(\mathbf{r}')}{|\mathbf{r} - \mathbf{r}'|} d\mathbf{r}' \quad (8)$$

The electron density  $\rho(\mathbf{r})$  and the potential  $U_{\text{n}}(\mathbf{r})$  created by all carbon ions,  $C^{4+}(1s^2)$ , were extracted from the Gaussian output file with the help of the Multiwfn

software [35]. The potential  $U_{\text{el}}(\mathbf{r})$  created by the delocalized electrons was calculated separately using the extracted electron density.

The jellium model treats the fullerenes  $\text{C}_{60}$  and  $\text{C}_{20}$  as spherically symmetric objects while a more precise *ab initio* calculation accounts for the real icosahedral symmetry of the molecules. Therefore, to draw an analogy between the two methods we averaged the exact electrostatic potential and the electron density over the directions of the position vector  $\mathbf{r}$ :

$$\begin{aligned}\bar{U}_{\text{tot}}(r) &= \bar{U}_{\text{n}}(r) + \bar{U}_{\text{el}}(r) , \\ \bar{U}_{\text{i}}(r) &= \frac{1}{4\pi} \int U_{\text{i}}(\mathbf{r}) d\Omega \quad (\text{i} = \text{tot}, \text{n}, \text{el}) , \\ \bar{\rho}(r) &= \frac{1}{4\pi} \int \rho(\mathbf{r}) d\Omega .\end{aligned}\tag{9}$$

The averaged electron density includes only delocalized electrons, while the inner electron orbitals are excluded from the consideration.

### 3. Numerical results

In this section we compare the results of the *ab initio* and the jellium model calculations for  $\text{C}_{60}$  and  $\text{C}_{20}$ . The fullerene  $\text{C}_{60}$  is discussed in detail below. The results for the  $\text{C}_{20}$  molecule and the comparison with  $\text{C}_{60}$  are discussed further in this section.

Using the methodology implemented in a number of papers [14, 17, 20, 23], we add a negative square well pseudopotential  $U_{\text{SW}}$  to the core potential (1):

$$U_{\text{core}}(r) \rightarrow \begin{cases} U_{\text{core}}(r) + U_{\text{SW}} & , R_1 \leq r \leq R_2 \\ U_{\text{core}}(r) & , \text{otherwise} \end{cases} .\tag{10}$$

The depth of the square well potential was chosen to obtain the same value of the outer shell ionization potential as the defined one from the quantum-chemical calculation. The pseudopotential  $U_{\text{SW}}$  is shown by the dashed red curve in the lower panel of figure 3.

Single-electron energy spectra obtained from the *ab initio* calculation and within the jellium model are presented in figure 1. Ionization potentials of several outer shells (6g, 10m and 7h) are in a good agreement with the *ab initio* results while the rest part of the jellium spectrum is significantly broadened and differs from the more precise calculation. It should be mentioned that none of the various jellium-based calculations of  $\text{C}_{60}$  that have been performed earlier [14, 17, 18, 19, 22, 23] can produce the quantitative agreement of the single-electron spectrum with that one obtained from the more precise *ab initio* calculation.

Radial density of the delocalized electrons obtained within the two approaches is presented in figure 2. It is shown that the standard jellium model without any corrections (dashed red curve) fails to represent the results of the *ab initio* calculation (black curve). The additional square well pseudopotential does not modify the density distribution significantly (solid red curve).

As it is shown in figures 1 and 2, the jellium model with a simple additional pseudopotential represents neither the single-electron energy spectrum nor the electron density distribution. As opposed to more precise quantum chemistry methods, the jellium model does not take into account chemical features of the fullerene, such as hybridization of atomic orbitals in the formation of chemical bonding. However, the

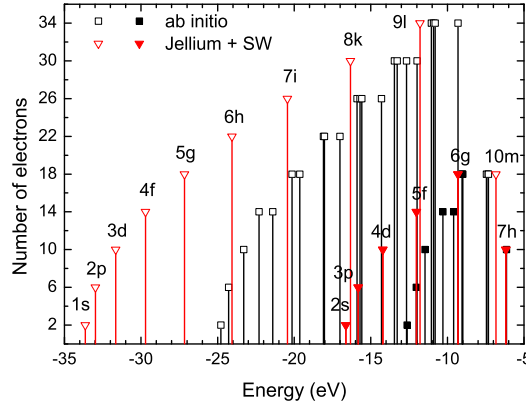


**Figure 1.** Single-electron energy levels of  $C_{60}$  obtained from the *ab initio* calculation (empty and filled squares) and within the jellium model with an additional square well (SW) pseudopotential (empty and filled triangles). Nodeless  $\sigma$ - and single-node  $\pi$ -orbitals are labeled by empty and filled symbols, respectively.

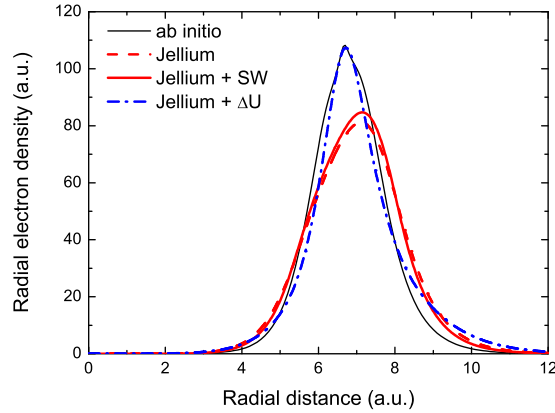


**Figure 2.** Radial electron density of  $C_{60}$  obtained from the *ab initio* calculation (solid black curve) and calculated by means of the jellium model: the standard one (dashed red curve), with the additional square well (SW) pseudopotential (solid red curve) and with the additional pseudopotential  $\Delta U$  (dash-dotted blue curve).

jellium model can be improved by means of a more sophisticated pseudopotential which will allow one to describe chemical properties of the real system. In the present paper, we introduce the correction as a difference between the total electrostatic potential of the system obtained from the *ab initio* calculation and the one obtained within the jellium model:

$$\Delta U(r) = U_{\text{tot}}^{\text{QC}}(r) - U_{\text{tot}}^{\text{jel}}(r). \quad (11)$$

The total potentials  $U_{\text{tot}}^{\text{QC}}(r)$  and  $U_{\text{tot}}^{\text{jel}}(r)$  of  $\text{C}_{60}$  as well as their difference  $\Delta U(r)$  are shown in figure 3.

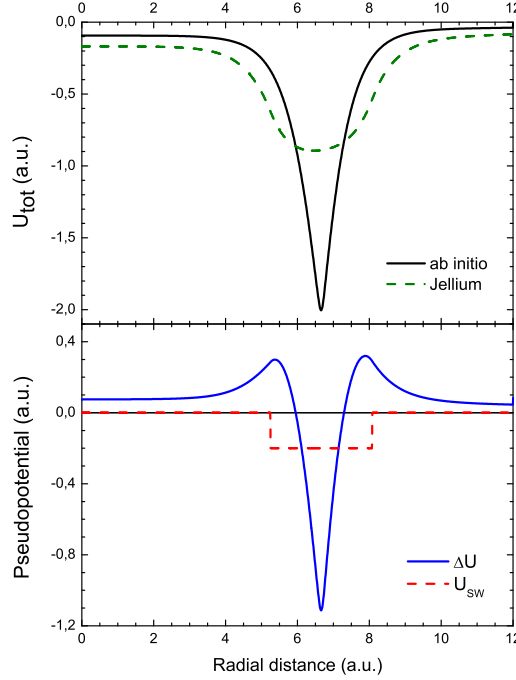


**Figure 3.** Upper panel: Total electrostatic potential of  $\text{C}_{60}$  obtained from the *ab initio* quantum chemistry calculation (solid curve) and within the jellium model (dashed curve). Lower panel: The difference  $\Delta U$  between the total electrostatic potential of  $\text{C}_{60}$  calculated by the *ab initio* methods and that one calculated within the jellium model (solid blue curve). The square well pseudopotential  $U_{\text{SW}}$  is also shown for the comparison (dashed red curve).

As opposed to the square well pseudopotential which effects equally on all electrons of the system,  $\Delta U$  is an alternating-sign pseudopotential (see the lower panel of figure 3), therefore it represents an attractive one in the vicinity of the fullerene ionic core and a repulsive one on the larger distances from the fullerene surface. That means that such potential would effect differently on the  $\sigma$ - and  $\pi$ -electrons of  $\text{C}_{60}$  which are located on the surface of the molecule and perpendicularly to it, respectively. Therefore, one can conclude that by means of a such potential it is possible to account, to some extent, for the hybridization properties of the fullerene.

The single-electron energy spectrum obtained within the "modified" jellium model with  $\Delta U$  taken as an additional pseudopotential is presented in figure 4. The modification allows one to obtain a better agreement of the jellium calculation with the *ab initio* one for the inner single-node  $2s \dots 5f$  orbitals. On the contrary, it shifts the  $6g$  and  $7h$  ionization potentials on 2.8 and 2.5 eV, respectively and still does not lead to a better quantitative agreement for the whole spectrum (see figure 4).

Introduction of the alternating-sign pseudopotential  $\Delta U$  allows one to improve significantly the electron density distribution (see the dash-dotted blue curve in figure 2). The difference between the *ab initio* calculated electron density and the one from

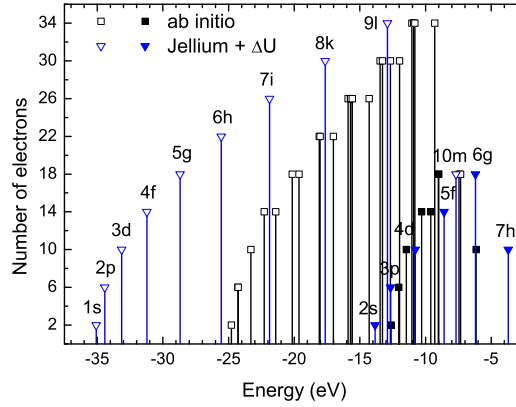


**Figure 4.** Single-electron energy levels of  $C_{60}$  obtained from the *ab initio* calculation (empty and filled squares) and within the modified jellium model with an additional pseudopotential  $\Delta U$  (empty and filled triangles). Nodeless  $\sigma$ - and single-node  $\pi$ -orbitals are labeled by empty and filled symbols, respectively.

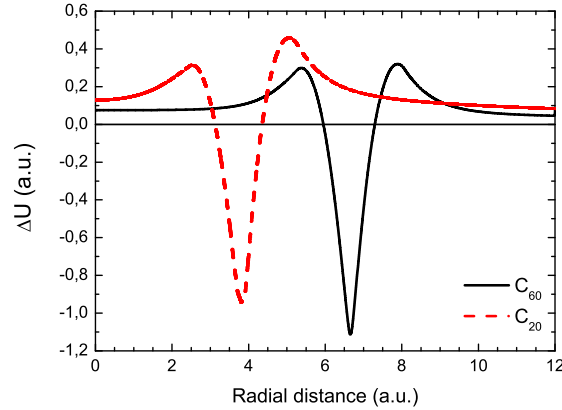


**Figure 5.** The additional pseudopotential  $\Delta U$  in case of  $C_{60}$  (solid curve) and  $C_{20}$  (dashed curve).

the jellium model calculation in the spatial region 8...12 a.u. may be a reason of the shift of 6g and 7h ionization potentials (see figure 4).

Below we present and discuss the results for the  $C_{20}$  molecule. Following the formalism described above for  $C_{60}$ , the additional pseudopotential  $\Delta U$  is introduced as a difference between the total electrostatic potential of  $C_{20}$  obtained from the *ab initio* quantum-chemical calculation and the one obtained within the jellium model. Figure 5 represents the correction  $\Delta U$  calculated for  $C_{60}$  and  $C_{20}$ . It is shown that  $\Delta U$  has a similar alternating-sign shape for both molecules but it is more asymmetric in the case of  $C_{20}$ .

The single-electron energy spectra of  $C_{20}$  are presented in figure 6. The



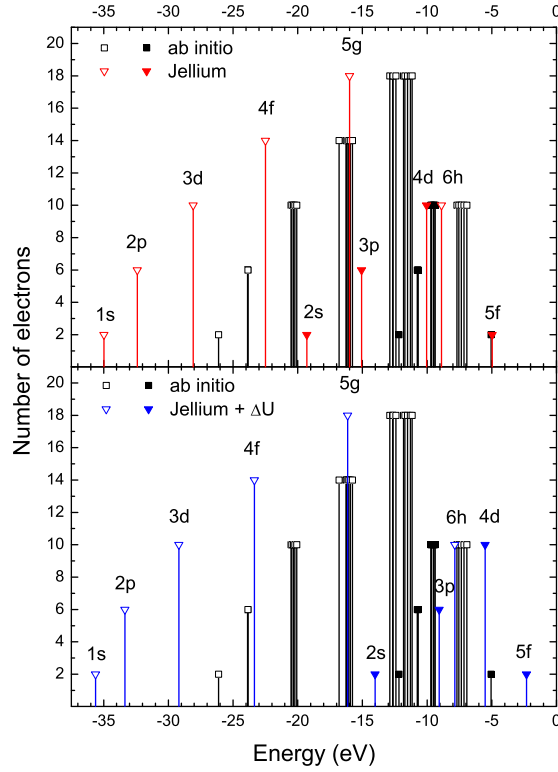


**Figure 6.** Single-electron energy levels of  $C_{20}$  obtained from the *ab initio* calculation (empty and filled squares) and within the jellium model (empty and filled triangles): the standard one (upper panel) and the modified one (lower panel). Nodeless  $\sigma$ - and single-node  $\pi$ -orbitals are labeled by empty and filled symbols, respectively.

pseudopotential  $\Delta U$  does not influence significantly on all nodeless orbitals while the single-node orbitals are shifted. This shift leads to a better agreement of the *ab initio* and jellium calculations for 2s and 3p shells but gives a wrong value for the outer 4d and 5f ionization potentials.

The additional pseudopotential  $\Delta U$  exert a similar influence on the electron density distribution of  $C_{20}$ , as in case of  $C_{60}$  (see figure 7). In comparison with a standard jellium model (dashed red curve), the modified one improves the density distribution in the vicinity of the fullerene core (dash-dotted blue curve) but the electron density is spread partly to the spatial region 5...9 a.u.

Having considered two different fullerenes within the spherical jellium model, one can conclude that the precise description of single-electron energy spectra of these systems by means of the jellium model is very difficult and elusive task, though such approach produces mostly the right sequence of energy levels. Additional pseudopotentials allow one to obtain the right value of the ionization potential only for several outer shells but do not alter the situation in whole significantly. At the same time, we suppose that improving the ground state density distribution with the introduced pseudopotential one can achieve higher accuracy while constructing the

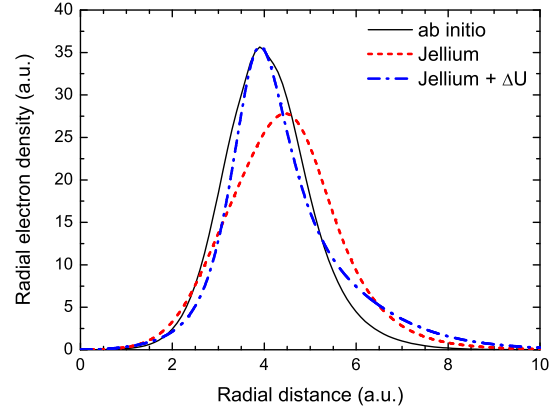


**Figure 7.** Radial electron density of  $C_{20}$  obtained from the *ab initio* calculation (solid curve) and calculated within the jellium model, the standard one (dashed curve) and with the additional pseudopotential  $\Delta U$  (dash-dotted curve).

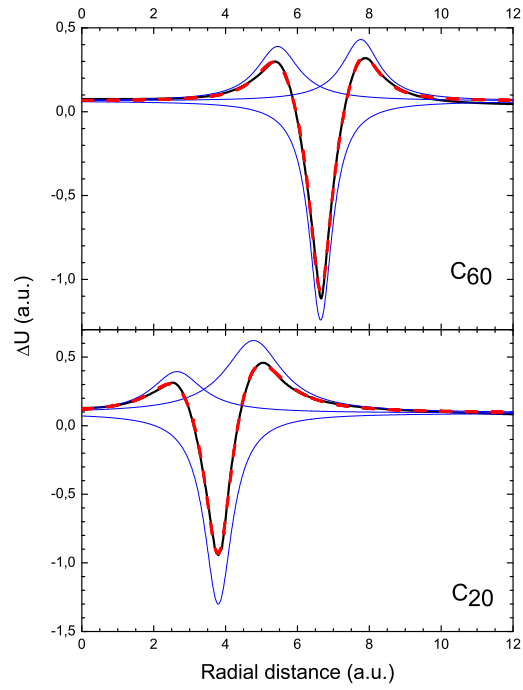


**Figure 8.** Pseudopotential  $\Delta U$  for the  $C_{60}$  (upper panel) and  $C_{20}$  (lower panel) compounds. The initial curve is presented by the thick solid (black) line, dashed (red) line represents the fitting curve constructed as a sum of three primitive Lorentz functions (thin blue lines).

photoionization amplitudes.

**Table 1.** Parameters of the Lorentz functions used for the fitting the pseudopotential  $\Delta U$  for  $C_{60}$  and  $C_{20}$ 

	$y_0$	$x_{c_1}$	$w_1$	$A_1$	$x_{c_2}$	$w_2$	$A_2$	$x_{c_3}$	$w_3$	$A_3$
$C_{60}$	0.064	5.453	1.425	0.727	6.647	0.785	-1.610	7.763	1.264	0.727
$C_{20}$	0.092	2.650	1.719	0.815	3.797	0.939	-2.053	4.779	1.934	1.606

The obtained pseudopotentials for  $C_{60}$  and  $C_{20}$  could be well fitted by three Lorentz functions. The result of the fitting procedure is presented in figure 8. Supposing  $\Delta U(r) \equiv y(x)$ , the resulting fitting function could be defined in the following form:

$$y(x) = y_0 + \sum_{i=1}^3 \frac{2A_i}{\pi} \frac{w_i}{4(x - x_{c_i})^2 + w_i^2}, \quad (12)$$

where  $y_0$  is the offset constant,  $x_c$  is the position of the peak maximum,  $w$  is the full width at half maximum and  $A$  is the normalization factor. The obtained values of these parameters are presented in table 1.

As it was shown above, the pseudopotential  $\Delta U$  has a more asymmetric form in case of  $C_{20}$  than in case of  $C_{60}$ , therefore it should effect differently on the  $\pi$ -electrons of these systems. Figure 9 represents the radial density of  $\pi$ -electrons in the  $C_{60}$  and  $C_{20}$  molecules obtained within the standard jellium model as well as the one augmented by  $\Delta U$ . The minimum of  $\pi$ -electron density distribution is located at 6.78 a.u. for  $C_{60}$  and 4.03 a.u. for  $C_{20}$ . These values are slightly shifted from the mean radius of the molecules, which equals 6.67 a.u. and 3.86 a.u., respectively. It is shown that due to the hybridization-related correction  $\Delta U$ ,  $\pi$ -electrons in both systems are distributed non-uniformly in the inner and outer regions of the molecules.

To estimate a relative degree of pressing out of the  $\pi$ -electrons to the outer region of the fullerene molecules, we normalized the density distributions by dividing them by the number of the  $\pi$ -electrons in each system. We also shifted the  $\pi$ -electron density of  $C_{60}$  to the one of  $C_{20}$  to match the minima of the curves. The result is presented in figure 10. It is shown that the profile of the  $\pi$ -electron density in  $C_{60}$  differs from the one in  $C_{20}$ . Due to the smaller radius of the molecule and a bigger curvature of the fullerene surface,  $\pi$ -electrons in  $C_{20}$  are pressed out more than in case of  $C_{60}$ . On the basis of this comparison, we suppose that for larger fullerenes, such as  $C_{240}$ ,  $\pi$ -electrons should be distributed more uniformly due to a smaller curvature of the surface of the molecule.

#### 4. Conclusion

To conclude, we have introduced a new type of the correction for description of the fullerenes  $C_{60}$  and  $C_{20}$  within the spherically symmetric jellium model. The correction is represented as an additional pseudopotential which originates from the difference between the precise *ab initio* calculation and the one within the jellium model. Due to an alternating-sign shape of the potential, it effects differently on  $\sigma$ - and  $\pi$ -electrons of the system. Therefore, this potential allows one to account for the  $sp^2$ -hybridization which occurs in the formation of fullerenes.

We have showed that the correction used improves significantly the electron density distribution comparing to the standard jellium model and the one with an

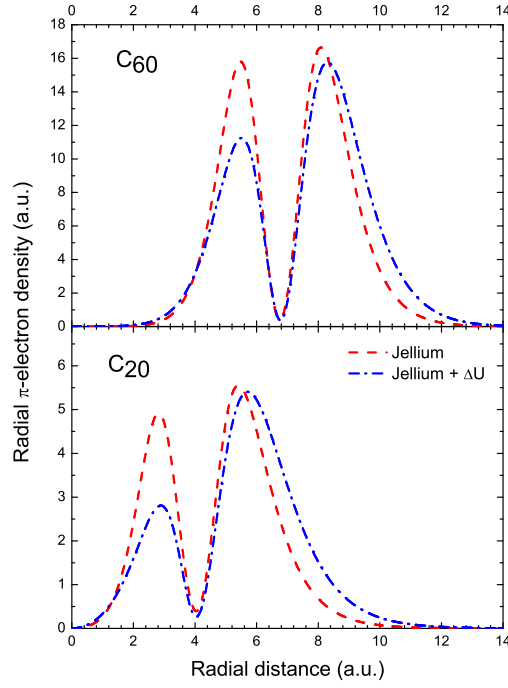


**Figure 9.** Radial density of  $\pi$ -electrons in  $C_{60}$  (upper panel) and  $C_{20}$  (lower panel) calculated within the standard jellium model (dashed red curve) and the modified jellium model with the presence of  $\Delta U$  (dash-dotted blue curve).

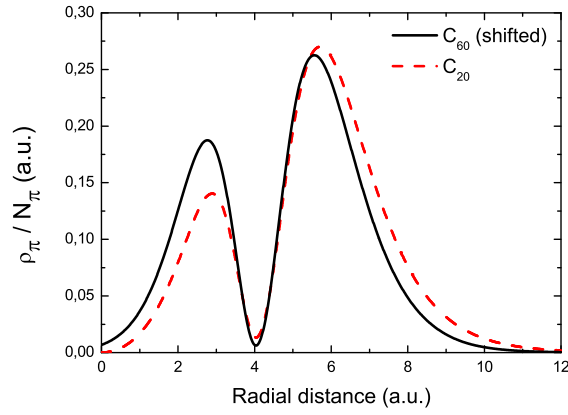


**Figure 10.** Radial  $\pi$ -electron densities,  $\rho_\pi$ , of the  $C_{60}$  and  $C_{20}$  fullerenes normalized by the number of the  $\pi$ -electrons,  $N_\pi$ , in each system. The density distribution of  $C_{60}$  is shifted to match the minima of the two curves (see the text for more explanation).

additional square well pseudopotential. Like the other previously used corrections, it does not allow to obtain a quantitative agreement with an *ab initio* calculation for the single-electron energy spectrum but produces the sequence of energy levels corresponding to the one following from the more precise quantum-chemical calculation.

The next step in this work could be the implementation of a more sophisticated model accounting for the electronic interactions in the system or the further improvement of the pseudopotential presented in this paper. An implementation of the presented formalism to larger fullerene molecules, nanotubes etc. is another topic for the further investigations.

## Acknowledgments

A.V.V. is grateful to Deutscher Akademischer Austauschdienst (DAAD) for the financial support.

## References

- [1] Kroto H W *et al* 1985 *Nature* **318** 162
- [2] Sattler K D 2010 *Handbook of Nanophysics: Clusters and Fullerenes* (Boca Raton: CRC Press)
- [3] Anilkumar P *et al* 2011 *Curr. Med. Chem.* **18** 2045
- [4] Melanko J B, Pearce M E and Salem A K 2009 *Nanotechnology in Drug Delivery*, ed M M de Villiers, P Aramwit and G S Kwon (New York: Springer) p 105
- [5] Bakry R, Vallant R M, Najam-ul-Haq M, Rainer M, Szabo Z, Huck C W and Bonn G K 2007 *Int. J. Nanomed.* **2** 639
- [6] Mroz P *et al* 2008 *Medicinal Chemistry and Pharmacological Potential of Fullerenes and Carbon Nanotubes* vol 1, ed F Cataldo and T Da Ros (New York: Springer Science+Business Media B.V.) p 79
- [7] Frisch M J *et al* 2009 Gaussian 09 Revision A.1, Gaussian Inc. Wallingford CT
- [8] Kaplan I G 1997 *Z. Phys. D* **40** 375
- [9] Rubio A, Alonso J A, Blase X, Balbas L C and Louie S G 1996 *Phys. Rev. Lett.* **77** 247
- [10] Solov'yov I A, Solov'yov A V and Greiner W 2004 *J. Phys. B: At. Mol. Opt. Phys.* **37** L137
- [11] Ekardt W 1984 *Phys. Rev. B* **29** 1558
- [12] Kharchenko V A, Ivanov V K, Ipatov A N and Zhyzhin M L 1994 *Phys. Rev. A* **50** 1459
- [13] Polozkov R G, Ivanov V K, Verkhovtsev A V and Solov'yov A V 2009 *Phys. Rev. A* **79** 063203
- [14] Yannouleas C and Landman U 1994 *Chem. Phys. Lett.* **217** 175
- [15] Guet C and Johnson W R 1992 *Phys. Rev. B* **45** 11283
- [16] Jänkälä K, Tchapyguine M, Mikkilä M-H, Björneholm O and Huttula M 2011 *Phys. Rev. Lett.* **107** 183401
- [17] Puska M J and Nieminen R M 1993 *Phys. Rev. A* **47** 1181
- [18] Wendin G and Wästberg B 1993 *Phys. Rev. B* **48** 14764
- [19] Yabana K and Bertsch G F 1993 *Phys. Scr.* **48** 633
- [20] Rüdel A, Hentges R, Becker U, Chakraborty H S, Madjet M E and Rost J-M 2002 *Phys. Rev. Lett.* **89** 125503
- [21] Kidun O, Fominykh N and Berakdar J 2004 *J. Phys. B: At. Mol. Opt. Phys.* **37** L321
- [22] Polozkov R G, Ivanov V K and Solov'yov A V 2005 *J. Phys. B: At. Mol. Opt. Phys.* **38** 4341
- [23] Madjet M E, Chakraborty H S, Rost J-M and Manson S T 2008 *J. Phys. B: At. Mol. Opt. Phys.* **41** 105101
- [24] Pavlyukh Y and Berakdar J 2010 *Phys. Rev. A* **81** 042515
- [25] Zhang Q L *et al* 1986 *J. Phys. Chem.* **90** 525
- [26] Krättschmer W, Fostiropoulos K and Huffman D R 1990 *Chem. Phys. Lett.* **170** 167
- [27] Goroff N S 1996 *Acc. Chem. Res.* **29** 77
- [28] Martins J L, Troullier N and Weaver J H 1991 *Chem. Phys. Lett.* **180** 457
- [29] Haddon R C, Brus L E and Raghavachari K 1986 *Chem. Phys. Lett.* **125** 459
- [30] Prinzbach H *et al* 2000 *Nature* **407** 60
- [31] Gianturco F A, Kashenock G Yu, Lucchese R R and Sanna N 2002 *J. Chem. Phys.* **116** 2811
- [32] Östling D, Apell P and Rosen A 1993 *Europhys. Lett.* **21** 539

- [33] Perdew J P and Zunger A 1980 *Phys. Rev. B* **23** 5048
- [34] Kohn W and Sham L J 1965 *Phys. Rev.* **140** A1133
- [35] Lu T and Chen F 2012 *J. Comp. Chem.* **33** 580